



## The Fire Modeling Intercomparison Project (FireMIP) for CMIP7

Fang Li<sup>1</sup>, David M. Lawrence<sup>2</sup>, Brendan M. Rogers<sup>3</sup>, Chantelle Burton<sup>4</sup>, Huilin Huang<sup>5</sup>, Yiquan Jiang<sup>6</sup>, Johannes W. Kaiser<sup>7</sup>, Matthew Kasoar<sup>8</sup>, Hanna Lee<sup>9</sup>, Ruby Leung<sup>10</sup>, Lars Nieradzik<sup>11</sup>, Aihui Wang<sup>1</sup>, Daniel S. Ward<sup>12</sup>, Ligeer Ce<sup>1,13</sup>, Yangchun Li<sup>1,13</sup>, Zhongda Lin<sup>1</sup>, Apostolos Voulgarakis<sup>14,7</sup>, and Yongkang Xue<sup>15</sup>

<sup>1</sup> State Key Laboratory of Earth System Numerical Modeling and Application, Institute of Atmospheric Physics, Chinese Academy of Sciences, Beijing, China

<sup>2</sup> NSF National Center for Atmospheric Research, Boulder, CO, USA

<sup>3</sup> Woodwell Climate Research Center, Falmouth, MA, USA

<sup>4</sup> Met Office Hadley Centre, Fitzroy Road, Exeter, UK

<sup>5</sup> University of Virginia, Charlottesville, VA, USA

<sup>6</sup> China Meteorological Administration–Nanjing University Joint Laboratory for Climate Prediction Studies, and Jiangsu Collaborative Innovation Center of Climate Change, School of Atmospheric Sciences, Nanjing University, Nanjing, China

<sup>7</sup> Atmosphere and Climate, The Climate and Environmental Research Institute NILU, Kjeller, Norway

<sup>8</sup> Leverhulme Centre for Wildfires, Environment and Society, Department of Physics, Imperial College London, London, UK

<sup>9</sup> Department of Biology, Norwegian University of Science and Technology, Trondheim, Norway

<sup>10</sup> Atmospheric, Climate, and Earth Sciences Division, Pacific Northwest National Laboratory, Richland, WA, USA

<sup>11</sup> Department of Physical Geography and Ecosystem Science, Lund University, Lund, Sweden

<sup>12</sup> Karen Clark & Company, Boston, MA, USA

<sup>13</sup> University of Chinese Academy of Sciences, Beijing, China

<sup>14</sup> School of Chemical and Environmental Engineering, Technical University of Crete, Chania, Greece

<sup>15</sup> Department of Geography, University of California Los Angeles, Los Angeles, CA, USA

*Correspondence to:* Fang Li (lifang@mail.iap.ac.cn)

**Abstract.** Fire is a global phenomenon and a key Earth system process. Extreme fire events have increased in recent years, and fire frequency and intensity are projected to rise across most regions and biomes, posing substantial challenges for ecosystems, the carbon cycle, and society. The Fire Model Intercomparison Project (FireMIP), launched in 2014, has contributed to advancing global fire modeling in Dynamic Global Vegetation Models (DGVs) and improving understanding of fire's local drivers and local impacts on vegetation and land carbon budgets through land offline (i.e., uncoupled from the atmosphere) simulations. We now bring FireMIP into Coupled Model Intercomparison Project Phase 7 (CMIP7) to: (1) evaluate fire simulations in state-of-the-art fully coupled Earth system models (ESMs); (2) assess fire regime changes in the past, present, and future, and identify their primary natural and



10 anthropogenic forcings and causal pathways within the Earth system, including the associated  
 uncertainties; and (3) quantify the impacts of fires and fire changes on climate, ecosystems, and society  
 across Earth system components, regions, and timescales, and elucidate the underlying mechanisms.  
 FireMIP in CMIP7 will advance the fire and fire-related modeling in fully coupled ESMs, and provide a  
 quantitative, detailed, and process-based understanding of fire's role in the Earth system by using models  
 15 that incorporate critical climate feedbacks and multi-model, multi-initial-condition, and CMIP7 multi-  
 scenario ensembles. This paper presents the motivation, scientific questions, experimental design and its  
 rationale, model inputs and outputs, and the analysis framework for FireMIP in CMIP7, providing  
 guidance for Earth system modeling teams conducting simulations and informing communities studying  
 fire, climate change, and climate solutions.

20

## 1. Introduction

Fire is a critical Earth system process, the primary form of terrestrial ecosystem disturbance on a global  
 scale, and has been present since the emergence of terrestrial plants around 400 million years ago (Scott  
 and Glasspool, 2006; Randerson et al., 2006; Bowman et al., 2009; Li et al., 2013). Each year, fire burns  
 25 over 400 Mha of vegetated land (Giglio et al., 2018; Chuvieco et al., 2019; Chen et al., 2023), releasing  
 2–4 Pg of carbon globally along with large amounts of aerosols, greenhouse gases, and tropospheric  
 ozone precursors (van der Werf et al., 2017; Wiedinmyer et al., 2023; Whaley et al., 2024; Kaiser et al.,  
 2025). Fire is regulated by climate, vegetation, and human activities, and feeds back to them in multiple  
 ways, both locally and remotely, across various temporal scales, forming intricate feedback loops (Bond-  
 30 Lamberty et al., 2007; Jiang et al., 2016; Li and Lawrence, 2017; Li et al., 2017, 2019, 2022; Jones et al.,  
 2022; Lou et al., 2023; Mao, 2024; Park et al., 2024; Harrison et al., 2025; Zhao et al., 2025). These  
 feedbacks may interact with potential tipping elements in vulnerable systems, such as permafrost thaw,  
 Amazon rainforest dieback, boreal forest dieback, and Arctic sea-ice loss (Lenton et al., 2019). Although  
 global burned area has declined over the past two decades (Andela et al., 2017), the frequency and  
 35 intensity of extreme fire events (Cunningham et al., 2025), as well as forest fire emissions (Zheng et al.,  
 2021), have increased. Importantly, global fire activity is projected to rise across most biomes, especially  
 under the high-emission scenario and in extratropical regions (Li, 2021; Yu et al., 2022; UNEP, 2022;  
 Sayedi et al., 2024; Bhattarai et al., 2025).



Earth system models (ESMs) simulate the processes and feedbacks within and among the  
40 atmosphere, ocean, land, sea ice, and biosphere, and are essential for understanding historical climate,  
environment, and ecosystems changes and for projecting the Earth's future (Scholze et al., 2013). ESMs  
have replaced climate models as the primary coupled models since the Coupled Model Intercomparison  
Project Phase 6 (CMIP6) (Dunne et al., 2025). Due to the critical role of fire in the Earth system, most  
ESMs now incorporate fire modeling. In CMIP6, 19 models submitted outputs of fire variables (Li et al.,  
45 2024a) versus 9 in CMIP5 (Kloster et al., 2017), and this number is expected to grow further in CMIP7.  
Furthermore, many ESMs have updated their fire schemes (e.g., Li et al., 2024b; Teixeira et al., 2025;  
Oberhagemann et al., 2025). Assessing the performance of CMIP7 ESMs in simulating fire and related  
variables is crucial for advancing fire-related process modeling.

Several studies have investigated fire changes across the past, present, and future and their local  
50 drivers. Over the past decades, global fire-regime changes are found to be driven mainly by human fire  
suppression (both direct and indirect, the latter through land-use-induced reduction in fuel continuity),  
enhanced by rising CO<sub>2</sub> levels that increase fuel load through CO<sub>2</sub> fertilization, and increasingly  
influenced by climate change (Andela et al., 2017; Li et al., 2018, 2019; Teckentrup et al., 2019; Burton  
et al., 2024; Scholten et al., 2024; Verjans et al., 2025). For the future, studies project an overall  
55 increase in global fire activity under CMIP5 and CMIP6 scenarios, particularly under the high emission  
scenario, mainly due to climate change including warming and increased lightning in Arctic-boreal  
regions and drying in the tropics (Kloster et al., 2017; Chen et al., 2021; Li, 2021; Wu et al., 2022;  
Byrne et al., 2024; Sayedi et al., 2024). Nevertheless, substantial uncertainties remain in the simulation  
of historical and future fire changes (Kloster et al., 2017; van Marle et al., 2017; Li et al., 2019; Li,  
60 2021; Hamilton et al., 2024). In CMIP7, the Scenario Model Intercomparison Project (ScenarioMIP)  
provides updated future scenarios that are more plausible than those in CMIP6, along with forcing  
datasets (van Vuuren et al., 2025). In addition, many studies have used simulations from the Detection  
and Attribution Model Intercomparison Project (DAMIP) experiments in CMIP6 to attribute the impact  
of anthropogenic and natural forcings on climate (IPCC, 2021; Gillett et al., 2025), but far fewer have  
65 examined the downstream impacts on wildfires, and those that do are focused on the western United  
States (e.g., Zhuang et al., 2021). How fire regimes will change under the CMIP7 scenarios and how  
anthropogenic and natural forcings have shaped historical global fire changes through climate and  
ecosystem processes remain unknown.



Fire impacts on the Earth system remain poorly quantified and understood. First, earlier studies primarily focused on specific components, such as biomass-burning effects on land carbon budgets or the radiative forcing and climate impacts of fire aerosols (Lasslop et al., 2019). Many other important fire impact processes, especially those across multiple Earth system components, are still unknown, for example, the global land-atmosphere-ocean carbon cycle, CH<sub>4</sub> emissions through affecting permafrost and wetland and their evolution in the atmosphere. Second, even for those processes that have been quantified, earlier estimates are likely inaccurate due to neglecting some critical climate feedbacks. Earlier studies quantified the fire impacts on land carbon and vegetation using land models driven by prescribed meteorological forcing, thereby neglecting fire-induced changes in surface climate (e.g., Li et al., 2014; Li and Lawrence, 2017; Ward et al., 2018; Arora and Melton, 2018; Lasslop et al., 2020; Pellegrini et al., 2023; Seo and Kim, 2023). Some coupled simulation studies adopted prescribed sea surface temperatures (SSTs) and/or sea ice coverage (e.g., Jiang et al., 2016; Grandey et al., 2016; Li et al., 2017a, b; Zou et al., 2020; Xu et al., 2021; Tian et al., 2022; Zhong et al., 2024; Blanchard-Wrigglesworth et al., 2025), which likely underestimated fire impacts due to the lack of air-sea interactions and sea-ice-albedo feedbacks (Jiang et al., 2020). Conversely, studies using a slab-ocean model, which lack horizontal heat transport, deep-water exchange, and ocean dynamics, may overestimate fire impacts (e.g., Jiang et al., 2020; Li et al., 2022; Zhao and Suzuki, 2019). Models without aerosol–cloud interactions (ACIs) have produced biased, sometimes even opposite-sign, fire-aerosol effects (e.g., Tosca et al., 2013; Yue and Unger, 2018; Li, 2020; Xu et al., 2021). Third, earlier coupled studies relied on a single model or a single initial-condition simulation, limiting characterization of model uncertainty and internal climate variability. For example, differences in the strength of ACIs or aerosol–radiation interactions can produce large inter-model spread in estimated net fire-aerosol effects, ranging from net cooling to net warming (Landry et al., 2017; Jiang et al., 2020; Zhong et al., 2024; Blanchard-Wrigglesworth et al., 2025). Moreover, small perturbations to initial conditions can influence simulated climate states for decades to even over a century (Kay et al., 2015). Multi-model, multi-initial-condition, fully coupled simulations with critical climate feedbacks from CMIP7 therefore offer a unique opportunity to more robustly quantify fire’s local and remote impacts across Earth system components and timescales, reveal the underlying mechanisms, and characterize the associated uncertainties.



The Fire Model Intercomparison Project (FireMIP), an international initiative launched in 2014, has worked to improve global fire modeling in DGVMs, understand local drivers of fires, and assess the influence of fires on vegetation, land carbon budgets, and, since 2020, on land and socioeconomic sectors as part of the Inter-Sectoral Impact Model Intercomparison Project (ISIMIP) (Hantson et al., 2016; Rabin et al., 2017; Frieler et al., 2024). Now integrated into CMIP7, FireMIP advances the study of fire's role in the Earth system using coupled model simulations. It contributes to improving fire and fire-related simulations in ESMs and addresses critical challenges in understanding fire dynamics, drivers, and impacts. CMIP7 FireMIP is also expected to provide useful insights for fire management, carbon accounting, air quality management, public health, land-use planning, and biodiversity protection. These insights link Earth system science to evidence-based policy making for risk management, ecosystem conservation, and sustainable development.

With the motivation and context outlined above, we describe in the following sections the scientific questions (Section 2), experimental design and rationale (Section 3), input and output variables (Section 4), and recommended analyses (Section 5), and conclude with the expected contributions to CMIP7 (Section 6).

## 2. Scientific Questions

FireMIP in CMIP7 aims to address three fundamental fire-related scientific questions (Fig. 1):

- (1) How well do state-of-the-art ESMs simulate global and regional fires?
- Li et al. (2024) evaluated fire simulations from CMIP6 ESMs and found that they had addressed three critical issues identified in CMIP5: (1) simulated global burned area being less than half of observations, (2) failure to reproduce the high burned area fraction observed in Africa, and (3) very weak fire seasonal variability. However, CMIP6 ESMs still underestimate the recent decline trend in global burned area, fail to capture the spring fire peak in the Northern mid-latitudes, and perform poorly in the Arctic-boreal zone. Since CMIP6, modeling groups have updated their ESMs (with fire-scheme improvements in some models), and more models will provide fire outputs in CMIP7. The first scientific question is therefore designed to assess how well state-of-the-art ESMs simulate fires, whether CMIP6 issues have been resolved, and what remaining or new issues emerge in CMIP7. It further aims to identify biases in fire and fire-related variables to guide future improvements in modeling fire-carbon-climate feedbacks, and



to support model selection and bias correction for more reliable assessments of fire changes, drivers, and impacts addressed in Questions 2 and 3.

130 (2) How have fire regimes changed in the past, how will they change in the future, and what are the dominant drivers of these changes?

This question investigates temporal and spatial changes in fire activity across the past, present, and future, along with the associated uncertainties. It examines the influence of natural and anthropogenic forcings on changes in fire regimes and, for anthropogenic forcings, further isolates the roles of greenhouse gases, 135 aerosols, and land-use change. By comparing these effects, the dominant forcings and their causal pathways within the Earth system can be identified.

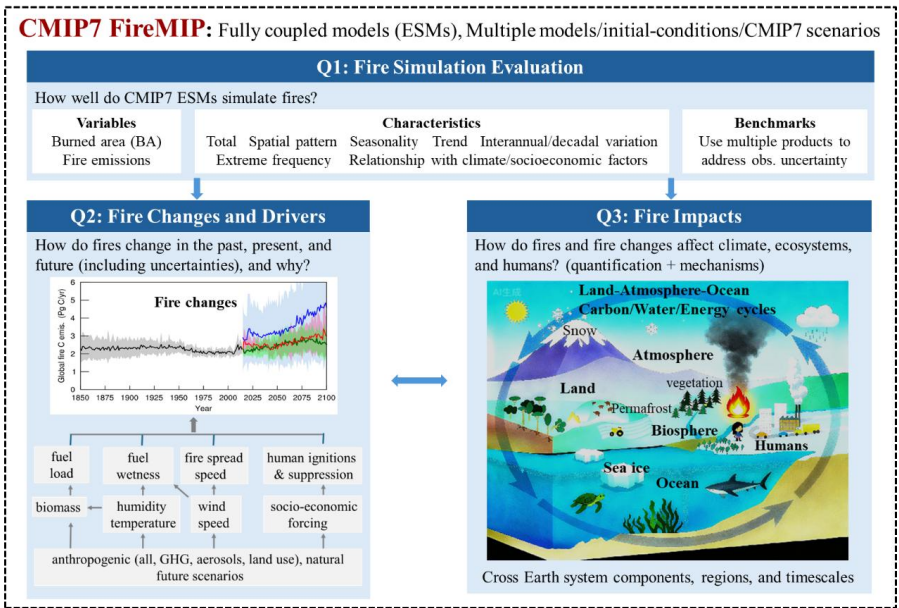


**Figure 1.** Scientific questions and proposed analyses for FireMIP in CMIP7. The fire-change panel is 140 adapted from Li (2021).

(3) How do fires and fire changes impact the climate, ecosystems, and humans?

This question explores the impacts of fires and changes in fire regimes on the land-atmosphere-ocean carbon, water, and energy cycles; vegetation distribution and structure; atmospheric composition, 145 chemistry, and circulation; surface climate (e.g., temperature, precipitation, humidity, wind speed); the



cryosphere (permafrost extent and active-layer depth, sea ice extent and thickness, snow cover and depth);  
air quality; and human activities. It also investigates the associated uncertainties, and the feedback  
mechanisms that cascade across Earth-system components. For example, it examines how fires influence  
climate and the carbon cycle through changes in land ecosystems and emissions of aerosols and trace  
gases, and how these changes, in turn, affect the spatial and temporal variability of fires. Addressing this  
question can also help clarify the potential role of fires in triggering or amplifying tipping-point  
transitions in boreal forests, the Amazon rainforest, permafrost, and Arctic sea ice.

### 3. Experimental design

CMIP7 FireMIP comprises three experiment groups (Table 1) designed to address the scientific questions  
outlined above. The design follows the principle of minimizing computational burden while effectively  
addressing the scientific questions, aiming to encourage broad participation from the modeling  
community, given that fully coupled ESM runs are very expensive. The tier-1 (required) experiments in  
Groups 1 and 2 come from CMIP7 Diagnostic, Evaluation and Characterization of Klima (DECK) and  
Assessment Fast Track (AFT) experiments. To participate in FireMIP, modeling groups must output two  
fire variables (i.e., burned area fraction and fire carbon emissions) from these simulations. Group 3 (Fire  
impacts) experiments are specific to FireMIP. Modeling groups are required to provide the hist-no-fire  
simulation and are encouraged to conduct one to three additional Group 3 experiments based on scientific  
interest and available resources. Running at least three initial-condition ensemble members for each  
experiment is strongly recommended to improve the robustness of the assessment, given the role of  
internal climate variability, and is consistent with DECK and AFT requirements.

Group 1 experiments are used to evaluate fire simulations and identify biases. The experiments  
include concentration-driven (historical) or emission-driven (esm-historical) coupled model simulations,  
and historical land model offline simulations (land-hist). Fire simulations in coupled models will be  
assessed to identify improvements compared to CMIP6 and to highlight issues that will guide further  
model development. Besides, the possible sources of improvement and bias (from land modeling,  
atmosphere modeling, or air-land coupling) can be identified by comparing coupled (historical or esm-  
historical) with land only (land-hist) simulations.



175

**Table 1.** Description of CMIP7 FireMIP experiments.

Group	Experiment ID	Description	Priority
1. Fire Simulation Evaluation	(1.1) historical/esm-historical (DECK)	1850–2021 historical concentration- or emission (esm)-driven coupled simulations	1
	(1.2) land-hist (AFT; LMIP tier-1)	1850–2021 offline land-model simulations	3
	(2.1) scen7-hc/esm-scen7-h scen7-mc/esm-scen7-m scen7-mlc/esm-scen7-ml scen7-lc/esm-scen7-l (AFT; ScenarioMIP tier-1)	2022–2100 concentration-driven or emission- driven coupled simulations under high (h, policy failure), medium (m, current policy), medium-low (ml, delayed mitigation policy), and low (l, Paris Agreement) emission scenarios	1
2. Fire Changes and Drivers	(2.2) hist-nat (AFT; DAMIP tier-1)	same as historical/esm-historical, with solar and volcanic forcings time-varying; other forcings fixed in 1850	1
	(2.3) hist-aer & hist-GHG (AFT; DAMIP tier-1) hist-lu (DAMIP tier-1)	same as historical/esm-historical, but with time-varying anthropogenic aerosols (hist-aer), greenhouse gases (hist-GHG), and land use (hist-lu), while other forcings fixed in 1850	2
	(2.4) scen7-vlloc/esm-scen7-vllo scen7-vlhoc/esm-scen7-vlho (AFT; ScenarioMIP tier-1)	2022–2100 coupled simulations under very low emissions after limited overshoot (vllo) and high overshoot (vlho) scenarios	3
	(3.1) hist-no-fire	1850–2021 historical coupled simulations with fires set to zero thereafter	1
	(3.2) hist-no-fireaero	branching from historical/esm-historical no later than 1920, with fire aerosols set to zero thereafter	2
2 Fire Impacts	(3.3) scen7-h-no-firechange	2022–2060 simulations as scen7-h, but with fires fixed at the 2001–2020 average	2
	(3.4) scen7-h-no-fireaerochange	2022–2060 simulations as scen7-h, but with fire aerosol emission fixed at the 2001–2020 average	2

Priority: 1 (required); 2 (recommended); 3 (optional)

Group 2 experiments are used to assess fire changes and drivers. These experiments include: (2.1)

180 simulations for 2022–2100 under high (h, policy failure), medium (m, current policy), medium-low (ml,





delayed mitigation policy), and low (l, aligned with Paris agreement) emission scenarios; and (2.2) a historical sensitivity simulation (hist-nat) similar to historical and esm-historical, driven by time-varying solar and volcanic forcings, with all other forcings fixed at their 1850 levels. In addition, lower-priority simulations in FireMIP include (2.3) 2022–2100 simulations under very low emissions after limited overshoot (vllo) and high overshoot (vlho), and (2.4) 1850–2022 simulations as historical and esm-historical with only anthropogenic aerosols (hist-aer), greenhouse gases (hist-GHG), and land use (hist-lu) varying in time, with other forcings fixed at 1850 levels.

Experiments (2.1) and (2.3), together with the historical and esm-historical simulations in Group 1, are used to assess how fire and fire emissions have changed during the historical period and how they will evolve under current-policy and failed-policy futures, as well as under varying levels of mitigation-policy success. Comparing experiments (2.2) and (2.4) with the historical and esm-historical simulations enables the assessment of how natural and anthropogenic forcings influence fires and isolates the effects of anthropogenic forcings, including aerosols, greenhouse gases, and land use.

Group 3 experiments are designed to quantify the impacts of fires, fire aerosols, future fire changes, and future changes in fire aerosols, respectively, and to explore the underlying mechanisms. Among them, (3.1) hist-no-fire is a 1850–2021 simulation without fires. In this experiment, burned area in the code should be set to zero, and any fire-induced emissions that are not simulated and passed to the atmosphere model need to be set to zero in the input data. CanESM simulations indicate that the global vegetation carbon pool and land surface air temperature require approximately 150–200 years and nearly 50 years, respectively, to reach their new no-fire equilibria after fires are switched off (V. K. Arora, 2025, personal communication). Therefore, starting the experiment from a 1850 no-fire spin-up is strongly recommended, to cleanly isolate present-day fire impacts (i.e., to avoid contamination by artificial trends caused by climate and carbon adjustment before equilibrium is reached). Experiment (3.2) hist-no-fireaero branches from the historical or esm-historical simulation no later than 1920, with fire-aerosol emissions set to zero thereafter. The year 1920 is chosen to provide at least 70 years of no-fire-aerosol spin-up, allowing the isolation of present-day fire-aerosol impacts. The spin-up length is informed by evidence that the global water cycle in CESM2 reaches no-fire-aerosol equilibrium after about 70 years (Li et al., 2022), and that the global vegetation and soil carbon pools require roughly 50 and 80 years, respectively, to equilibrate or show only minor slow changes in the CMIP6 global deforestation experiment (Boysen et al., 2020). Comparing the present-day averages, seasonality, recent



trends, and decadal/interannual variations of target variables from experiments (3.1) and (3.2) with the historical or esm-historical simulations enables the assessment of fire impacts and fire-aerosol impacts, respectively.

215 Additionally, Experiments (3.3) scen7-h-nofirechange is a 2022–2060 simulation, the same as scen7-h, but with burned area and fire emissions fixed at their 2001–2020 average; this requires burned area to be prescribed as an input field using each model’s own 2001–2020 average derived from its historical simulations, and in models without interactive fire-emission modules, fire emissions in the 2022–2060 input files must likewise be replaced with the 2001–2020 average. Experiment (3.4) scen7-h-no-fireaerochange is a 2022–2060 simulation, the same as scen7-h, but with fire aerosol  
 220 emissions in the inputs fixed at the 2001–2020 average, which is not applicable to ESMs with interactive fire-emission modules. Comparing Experiments (3.3) and (3.4) with the scen7-h simulations for 2022–2060 facilitates assessing the impacts of future changes in fires and fire aerosols, respectively, under a high-emission scenario.

#### 4. Inputs and outputs

##### 225 4.1 Inputs

Fire-specific inputs include: (1) population density, for modeling ignitions and human fire suppression; (2) lightning frequency for natural ignitions; (3) GDP for human fire suppression; (4) peatland area fraction, for peat fire modeling; (5) peak month of agricultural fires for timing of agricultural waste burning; and (6) fire-sourced trace gas and aerosol emissions representing part of fire impacts.

230 Not all ESMs require or use all six inputs. For example, ESMs without modeling direct human effects on fires likely do not need population density, GDP, or peak month of agricultural fires. Similarly, models that do not simulate peat fires do not require peatland area fraction. For ESMs that activate the interactive fire-emission module (i.e., simulate fire emissions and pass to the atmospheric model) and model lightning, prescribed fire emissions and lightning frequency are not needed.

235 Historical gridded population density data (1850–2025; Paprotny and Hawker, 2025) and fire emission data (1750–2023; van Marle and van der Werf, 2025) are provided by CMIP7 forcing group and available through [https://input4mips-cvs--350.org.readthedocs.build/en/350/database-views/input4MIPs\\_delivery-summary.html](https://input4mips-cvs--350.org.readthedocs.build/en/350/database-views/input4MIPs_delivery-summary.html). Future population density and fire aerosol emission datasets are under development. Because CMIP7 will not provide forcing data for inputs (2–5), models may use



240 their default settings.

## 4.2 Output variables

The variables requested by CMIP7 FireMIP are classified into two categories: (1) fire variables and (2) fire driver and impact variables. The fire variables, specifically burned area fraction and fire carbon emissions, are the highest priority (Table 2). They are essential for evaluating fire simulations and  
 245 assessing fire-regime changes.

**Table 2.** CMIP7 FireMIP outputs: fire variables

Name	Description	Branded name	Unit	#Dims	Frequency
burntFractionAll	Burned Area Fraction	burntFractionAll_tavg -u-hxy-u	% mon <sup>-1</sup>	3	monthly
fFire	Fire Carbon Emissions	fFire_tavg-u-hxy-lnd	kg C m <sup>-2</sup> s <sup>-1</sup>	3	monthly

The fire driver and impact variables include land-atmosphere-ocean carbon cycle variables (Table  
 250 3) as well as other land (vegetation structure, vegetation distribution, land nitrogen fluxes and pools, and land hydrothermal, snow characteristics), atmosphere (meteorology, atmospheric circulation, physics, composition, and chemistry), and ocean and sea-ice variables (Table 4). These variables will be used to evaluate model accuracy in capturing fire-ecosystems and fire-climate relationships, and to investigate the drivers of fire-regime changes and fire impacts.

255 These fire driver and impact variables are selected because previous studies show that they (1) respond to natural and anthropogenic forcings, and can also influence fuel load, fuel flammability, and/or fire spread (IPCC, 2021; Gillett et al., 2025); (2) are significantly affected by fires at global or regional scales, e.g., land carbon budgets and vegetation (e.g., Bond-Lamberty et al., 2007; Li et al., 2014; Yue and Unger, 2018; Lasslop et al., 2020; Zou et al., 2020; Seo and Kim, 2023), land nitrogen  
 260 fluxes and pools (Beaudor et al., 2025), surface climate (e.g., Jiang et al., 2016; Li and Lawrence 2017; Li et al., 2017), land-atmosphere energy exchange (e.g., Li et al., 2017), water cycle (Li et al., 2022), CH<sub>4</sub> cycle (Tian et al., 2016), dust emissions (Yu and Ginoux, 2022), atmospheric composition and chemistry (e.g., Ward et al., 2012; Li et al., 2019; Jiang et al., 2020), large-scale atmospheric circulation (Li et al., 2022; Scholten et al., 2022), sea ice and snow (e.g., Li et al., 2022; Zhong et al., 2024),  
 265 permafrost (Talucci et al., 2025), sea-surface temperature (Li et al., 2022), and marine ecosystems (Liu et al., 2022; Riera and Pausas, 2023); (3) are likely affected by the fire-induced changes listed in (2)



(i.e., downstream variables), such as atmosphere and ocean carbon and energy; and (4) are needed to diagnose the response and influence mechanisms (i.e., intermediate variables), such as ocean currents.

270 **Table 3.** CMIP7 FireMIP outputs: land-atmosphere-ocean carbon cycle variables

Name	Description	Branded name	Unit	#Dims	Frequency
gpp	Gross Primary Productivity	gpp_tavg-u-hxy-lnd	kg C m <sup>-2</sup> s <sup>-1</sup>	3	monthly
ra	Autotrophic Respiration	ra_tavg-u-hxy-lnd	kg C m <sup>-2</sup> s <sup>-1</sup>	3	monthly
rh	Heterotrophic Respiration	rh_tavg-u-hxy-lnd	kg C m <sup>-2</sup> s <sup>-1</sup>	3	monthly
fLuc	Land-Use Change carbon emissions	fLuc_tavg-u-hxy-lnd	kg C m <sup>-2</sup> s <sup>-1</sup>	3	monthly
npp	Net Primary Productivity	npp_tavg-u-hxy-lnd	kg C m <sup>-2</sup> s <sup>-1</sup>	3	monthly
nep	Net Ecosystem Productivity	nep_tavg-u-hxy-lnd	kg C m <sup>-2</sup> s <sup>-1</sup>	3	monthly
nbp	Net Biospheric Productivity	nbp_tavg-u-hxy-lnd	kg C m <sup>-2</sup> s <sup>-1</sup>	3	monthly
cLeaf	Carbon mass in leaves	cLeaf_tavg-u-hxy-lnd	kg C m <sup>-2</sup>	3	monthly
cStem	Carbon Mass in stems	cStem_tavg-u-hxy-lnd	kg C m <sup>-2</sup>	3	monthly
cRoot	Carbon Mass in Roots	cRoot_tavg-u-hxy-lnd	kg C m <sup>-2</sup>	3	monthly
cProduct	Carbon Mass in Products of Land-Use Change	cProduct_tavg-u-hxy-lnd	kg C m <sup>-2</sup>	3	monthly
cVeg	Carbon Mass in Vegetation	cVeg_tavg-u-hxy-lnd	kg C m <sup>-2</sup>	3	monthly
cLitter	Carbon Mass in Litter	cLitter_tavg-u-hxy-lnd	kg C m <sup>-2</sup>	3	monthly
cSoil	Carbon Mass in Soil	cSoil_tavg-u-hxy-lnd	kg C m <sup>-2</sup>	3	monthly
co2	Mole Fraction of CO <sub>2</sub> in air	co2_tavg-p19-hxy-air	mol mol <sup>-1</sup>	3	monthly
fgco2	Surface Downward Mass Flux of Carbon as CO <sub>2</sub>	fgco2_tavg-u-hxy-sea	kg C m <sup>-2</sup> s <sup>-1</sup>	3	monthly
spco2	Surface Aqueous Partial Pressure of CO <sub>2</sub>	spco2_tavg-u-hxy-sea	Pa	3	monthly
dissic	Dissolved Inorganic Carbon Concentration	dissic_tavg-ol-hxy-sea	mol m <sup>-3</sup>	3	monthly
dissoc	Dissolved Organic Carbon Concentration	dissoc_tavg-ol-hxy-sea	mol m <sup>-3</sup>	3	monthly
intnpp	NPP by Phytoplankton	intpp_tavg-u-hxy-sea	Kg C m <sup>-2</sup>	3	monthly

The variables required for CMIP7 FireMIP are in the variable list of CMIP7 DECK and AFS experiments, with no additional requests specifically for FireMIP. It is acceptable for some variables to be absent if the model does not include the corresponding component or process, such as the ocean ecosystem, terrestrial nitrogen cycle, CH<sub>4</sub> cycle, groundwater, or air-quality (e.g., surface PM<sub>2.5</sub> and O<sub>3</sub> concentrations).

Some variables in Table 4 are listed with daily or hourly frequencies because corresponding



monthly variables are unavailable in the CMIP7 variable list. If modeling teams provide monthly outputs for these variables, that is acceptable. CMIP7 FireMIP does not have specific requirements for spatial resolution.

**Table 4.** CMIP7 FireMIP outputs: other land, atmosphere, ocean, and sea ice variables

Name	Description	Branded name	Unit	#Dims	frequency
Land					
lai	Leaf Area Index	lai_tavg-u-hxy-lnd	unitless	3	monthly
vegHeight	Height of Canopy	vegHeight_tavg-u-hxy-veg	m	3	monthly
treeFrac	Tree Cover Percentage	treeFrac_tavg-u-hxy-u	%	3	monthly
grassFrac	Grass Area Percentage	grassFrac_tavg-u-hxy-u	%	3	monthly
shrubFrac	Shrub Area Percentage	shrubFrac_tavg-u-hxy-u	%	3	monthly
cropFrac	Crop Area Percentage	cropFrac_tavg-u-hxy-u	%	3	monthly
baresoilFrac	Bare Soil Area Percentage	baresoilFrac_tavg-u-hxy-u	%	3	monthly
fNgasFire	Nitrogen Lost to the Atmosphere from Fire	fNgasFire_tavg-u-hxy-lnd	kg N m <sup>-2</sup> s <sup>-1</sup>	3	monthly
fNdep	Nitrogen deposition	fNdep_tavg-u-hxy-lnd	kg N m <sup>-2</sup> s <sup>-1</sup>	3	monthly
Fbnf	Biological Nitrogen Fixation	fBNF_tavg-u-hxy-lnd	kg N m <sup>-2</sup> s <sup>-1</sup>	3	monthly
fNleach	Nitrogen Loss to Leaching or Runoff	fNleach_tavg-u-hxy-lnd	kg N m <sup>-2</sup> s <sup>-1</sup>	3	monthly
fNup	Total Plant Nitrogen Uptake	fNup_tavg-u-hxy-lnd	kg N m <sup>-2</sup> s <sup>-1</sup>	3	monthly
nVeg	Vegetation Nitrogen Mass	nVeg_tavg-u-hxy-lnd	kg N m <sup>-2</sup>	3	monthly
nLitter	Nitrogen Mass in Litter	nLitter_tavg-u-hxy-lnd	kg N m <sup>-2</sup>	3	monthly
nSoil	Nitrogen Mass in Soil	nSoil_tavg-u-hxy-lnd	kg N m <sup>-2</sup>	3	monthly
nMineral	Soil Mineral Nitrogen	nMineral_tavg-u-hxy-lnd	kg N m <sup>-2</sup>	3	monthly
tsl	Soil temperature	tsl_tavg-sl-hxy-lnd	K	4	monthly
mrsol	Water Content of Soil Layer	mrsol_tavg-sl-hxy-lnd	kg m <sup>-2</sup>	4	monthly
mrso	Total Soil Moisture Content	mrso_tavg-u-hxy-lnd	kg m <sup>-2</sup>	3	monthly
evspsblveg	Canopy Evaporation	evspsblveg_tavg-u-hxy-lnd	kg m <sup>-2</sup> s <sup>-1</sup>	3	monthly
evspsblsoi	Soil Evaporation	evspsblsoi_tavg-u-hxy-lnd	kg m <sup>-2</sup> s <sup>-1</sup>	3	monthly
tran	Transpiration	tran_tavg-u-hxy-lnd	kg m <sup>-2</sup> s <sup>-1</sup>	3	monthly
evspsbl	Evapotranspiration	evspsbl_tavg-u-hxy-u	kg m <sup>-2</sup> s <sup>-1</sup>	3	monthly
mrro	Total Runoff	mrro_tavg-u-hxy-lnd	kg m <sup>-2</sup> s <sup>-1</sup>	3	monthly
mrros	Surface Runoff	mrros_tavg-u-hxy-lnd	kg m <sup>-2</sup> s <sup>-1</sup>	3	monthly
rivo	River Discharge	rivo_tavg-u-hxy-lnd	m <sup>3</sup> s <sup>-1</sup>	3	daily
friver	Water Flux into Sea Water from Rivers	friver_tavg-u-hxy-sea	kg m <sup>-2</sup> s <sup>-1</sup>	3	monthly
dgw	Change in Groundwater	dgw_tavg-u-hxy-lnd	kg m <sup>-2</sup>	3	daily



wtd	Water Table Depth	wtd_tavg-u-hxy-lnd	m	3	daily
prveg	Canopy Interception	prveg_tavg-u-hxy-lnd	kg m <sup>-2</sup> s <sup>-1</sup>	3	monthly
rlds	Surface Downwelling Longwave Radiation	rlds_tavg-u-hxy-u	W m <sup>-2</sup>	3	monthly
rsus	Surface Upwelling Shortwave Radiation	rsus_tavg-u-hxy-u	W m <sup>-2</sup>	3	monthly
rlus	Surface Upwelling Longwave Radiation	rlus_tavg-u-hxy-u	W m <sup>-2</sup>	3	monthly
hfls	Surface Upward Latent Heat Flux	hfls_tavg-u-hxy-u	W m <sup>-2</sup>	3	monthly
hfss	Surface Upward Sensible Heat Flux	hfss_tavg-u-hxy-u	W m <sup>-2</sup>	3	monthly
hfds	Downward Heat Flux at Sea Water Surface	hfds_tavg-u-hxy-sea	W m <sup>-2</sup>	3	monthly
hfdsl	Ground heat flux	hfdsl_tavg-u-hxy-lnd	W m <sup>-2</sup>	3	3-hourly
rsdsdiff	Surface Diffuse Downwelling Shortwave Radiation	rsdsdiff_tavg-u-hxy-u	W m <sup>-2</sup>	3	daily
snm	Surface Snow Melt	snm_tavg-u-hxy-lnd	kg m <sup>-2</sup> s <sup>-1</sup>	3	monthly
snd	Snow Depth	snd_tavg-u-hxy-lnd	m	3	monthly
snc	Snow Area Percentage	snc_tavg-u-hxy-lnd	%	3	monthly
snw	Surface Snow Amount	snw_tavg-u-hxy-lnd	kg m <sup>-2</sup>	3	monthly
Atmosphere					
pr	Precipitation	pr_tavg-u-hxy-u	kg m <sup>-2</sup> s <sup>-1</sup>	3	monthly
tas	Near-surface air temperature	tas_tavg-h2m-hxy-u	K	3	monthly
tasmax	Daily Maximum Near-Surface Air Temperature	tas_tmax-h2m-hxy-u	K	3	monthly
tasmin	Daily Minimum Near-Surface Air Temperature	tas_tmin-h2m-hxy-u	K	3	monthly
sfcWind	Near-Surface Wind Speed	sfcWind_tavg-h10m-hxy-u	m s <sup>-1</sup>	3	monthly
hurs	Near-Surface Relative Humidity	hurs_tavg-h2m-hxy-u	%	3	monthly
psl	Sea Level Pressure	psl_tavg-u-hxy-u	Pa	3	monthly
zg	Geopotential Height	zg_tavg-p19-hxy-air	m	4	monthly
ua	Eastward Wind	ua_tavg-p19-hxy-air	m s <sup>-1</sup>	4	monthly
va	Northward Wind	va_tavg-p19-hxy-air	m s <sup>-1</sup>	4	monthly
ta	Air Temperature	ta_tavg-p19-hxy-air	K	4	monthly
hus	Specific Humidity	hus_tavg-p19-hxy-u	l	4	monthly
cldnvi	Column Integrated Cloud Droplet Number	cldnvi_tavg-u-hxy-u	m <sup>-2</sup>	3	monthly
clt	Total Cloud Cover Percentage	clt_tavg-u-hxy-u	%	3	monthly



rsdt	TOA Incident Shortwave Radiation	rsdt_tavg-u-hxy-u	$\text{W m}^{-2}$	3	monthly
rsdcs	Downwelling Clear-Sky Shortwave Radiation at the surface and TOA	rsdcs_tavg-alh-hxy-u	$\text{W m}^{-2}$	4	monthly
loadbc	Load of BC	loadbc_tavg-u-hxy-u	$\text{kg m}^{-2}$	3	daily
loadpoa	Load of Dry Aerosol Primary Organic Matter	loadpoa_tavg-u-hxy-u	$\text{kg m}^{-2}$	3	daily
loadso4	Load of SO <sub>4</sub>	loadso4_tavg-u-hxy-u	$\text{kg m}^{-2}$	3	monthly
od550bb	Aerosol Optical Depth at 550nm Due to Biomass Burning	od550bb_tavg-u-hxy-u	1	3	monthly
od550bc	Black Carbon Optical Thickness at 550nm	od550bc_tavg-u-hxy-u	1	3	monthly
od550oa	Total Organic Aerosol Optical Depth at 550nm	od550oa_tavg-u-hxy-u	1	3	monthly
lwp	Liquid Water Path	lwp_tavg-u-hxy-u	$\text{kg m}^{-2}$	3	monthly
sfo3	O <sub>3</sub> Volume Mixing Ratio in Lowest Model Layer	o3_tavg-h2m-hxy-u	$\text{mol mol}^{-1}$	3	hourly
sfp25	PM <sub>2.5</sub> Mass Mixing Ratio in Lowest Model Layer	sfp25_tavg-h2m-hxy-u	$\text{kg kg}^{-1}$	3	daily
emico	Total Emission Rate of CO	emico_tavg-u-hxy-u	$\text{kg m}^{-2} \text{ s}^{-1}$	3	monthly
emibbch4	total emission of CH <sub>4</sub> from all biomass burning	emibbch4_tavg-u-hxy-u	$\text{kg m}^{-2} \text{ s}^{-1}$	3	monthly
emich4	Total Emission Rate of CH <sub>4</sub>	emich4_tavg-u-hxy-u	$\text{kg m}^{-2} \text{ s}^{-1}$	3	monthly
ch4global	Global Mean Mole Fraction of CH <sub>4</sub>	ch4_tavg-u-hm-u	1E-09	1	monthly
eminox	Total Emission Rate of NO <sub>x</sub>	eminox_tavg-u-hxy-u	$\text{kg m}^{-2} \text{ s}^{-1}$	3	monthly
emibvoc	Total Emission Rate of Biogenic NMVOC	emibvoc_tavg-u-hxy-u	$\text{kg m}^{-2} \text{ s}^{-1}$	3	monthly
emidust	Total Emission Rate of Dust	emidust_tavg-u-hxy-u	$\text{kg m}^{-2} \text{ s}^{-1}$	3	monthly
Ocean and sea ice					
no3	Dissolved Nitrate Concentration	no3_tavg-ol-hxy-sea	$\text{mol m}^{-3}$	3	monthly
po4	Total Dissolved Inorganic Phosphorus Concentration	po4_tavg-ol-hxy-sea	$\text{mol m}^{-3}$	3	monthly
chl	Mass Concentration of Phytoplankton Expressed as Chlorophyll in Sea Water	chl_tavg-ol-hxy-sea	$\text{kg m}^{-3}$	3	monthly



talk	Total Alkalinity	talk_tavg-ol-hxy-sea	mol m <sup>-3</sup>	3	monthly
fsfe	Surface Downward Net Flux of Iron	fsfe_tavg-u-hxy-sea	mol m <sup>-2</sup> s <sup>-1</sup>	3	monthly
dfe	Dissolved Iron Concentration	dfe_tavg-ol-hxy-sea	mol m <sup>-3</sup>	3	monthly
uo	Sea Water X Velocity	uo_tavg-ol-hxy-sea	m s <sup>-1</sup>	4	monthly
vo	Sea Water Y Velocity	vo_tavg-ol-hxy-sea	m s <sup>-1</sup>	4	monthly
thetao	Sea Water Potential Temperature	thetao_tavg-ol-hxy-sea	degC	4	monthly
so	Sea Water Salinity	so_tavg-ol-hxy-sea	1E <sup>-03</sup>	4	monthly
tos	Sea Surface Temperature	tos_tavg-u-hxy-sea	°C	3	monthly
zos	Sea Surface Height Above Geoid	zos_tavg-u-hxy-sea	m	3	monthly
mloit	Ocean Mixed Layer Thickness	mloit_tavg-u-hxy-sea	m	3	monthly
msftyz	Ocean Meridional Overturning Mass Stream Function	msftm_tavg-ol-hys-sea	kg s <sup>-1</sup> or Sv	4	monthly
siconc	Sea-Ice Area Fraction	siconc_tavg-u-hxy-u	1	3	monthly
sithick	Sea-Ice Thickness	sithick_tavg-u-hxy-si	m	3	monthly

## 5. Recommended analysis

### 285 5.1 Fire simulation evaluation

The ability of CMIP7 ESMs to simulate global and regional total burned area and fire carbon emissions will be evaluated, as well as their spatial and temporal variability (including spatial pattern, recent and long-term historical trends, and phases of seasonal variability, magnitude of interannual and decadal variability), extreme fire frequency, and relationships between fires with climatic and socioeconomic factors (Fig. 1). Unlike offline simulations of land surface models and DGVMs, which are driven by observed climate data, coupled models in CMIP are free-running and driven solely by anthropogenic forcing. As a result, they are not designed to synchronize with the actual climate state of specific years or decades. Consequently, expecting a one-to-one match between CMIP-simulated and observed fires for any given year or decade is unrealistic. Instead, we recommend evaluating how fires respond to large-scale climate oscillations, such as ENSO and PDO for tropical fires, and AO/NAO for Arctic-boreal fires (Ward et al., 2016; Chen et al., 2017; Kim et al., 2020; Zhao et al., 2022; Li et al., 2024a).





Given the large uncertainties in global fire observations (Table 5; Li et al., 2024a; Kaiser et al., 2025), we recommend evaluating fire simulations against multiple benchmarks. For present-day burned area, benchmarks could include GFED5 (van der Werf et al., 2025), FireCCI5.1 (Chuvieco et al., 2019),  
300 FireCCI60 (Pettinari et al., 2025), and MODIS Collection 6.1 (Giglio et al., 2018). For present-day fire emissions, options include GFED5 (van der Werf et al., 2025), CAMS-GFAS1.2 (Kaiser et al., 2012), GFAS4HTAP (Kaiser et al., 2024; 2025), FINN2.5 (Wiedinmyer et al., 2023), FEER1 (Ichoku and Ellison, 2014), and QFED2.5 (Darmenov and da Silva, 2015).

305 **Table 5.** Summary description of satellite-based products as benchmarks for fire simulations

Name	Methods	Resolution	Period	Global total	reference
Burned Area					
GFED5	MODIS BA & MODIS, ATSR, VIIRS active fire counts	0.25° monthly	1997–2022	802 Mha yr <sup>-1 a</sup>	Chen et al. (2023)
FireCCI5.1	MODIS reflectance & active fire counts	0.25° monthly	2001–2020	473 Mha yr <sup>-1 a</sup>	Chuvieco et al. (2019)
FireCCI6	MODIS & Sentinel-3 reflectance; MODIS & VIIRS active fire counts	0.25° monthly	2003–2024	634 Mha yr <sup>-1 b</sup>	Pettinari et al. (2025)
MODIS C6.1	MODIS reflectance & active fire counts	0.25° monthly	2001–present	430 Mha yr <sup>-1 a</sup>	Giglio et al. (2018)
Fire emissions					
GFED5	fuel consumption, GFED5 burned area	0.25° monthly	1997–2022	3.4 Pg C yr <sup>-1 c</sup> 0.53 Pg CO yr <sup>-1 c</sup>	van der Werf et al. (2025)
CAMS-GFAS1.2	(GFED), MODIS FRP (GFAS), MODIS active	0.1° daily	2003–present	2.1 Pg C yr <sup>-1 a</sup> 0.36 Pg CO yr <sup>-1 a</sup>	Kaiser et al. (2012)
GFAS4HTAP1.2	fire counts (FINN), emis. Factor	0.1° daily	2003–2023	0.36 Pg CO yr <sup>-1 d</sup>	Kaiser et al. (2024)
FINN2.5		1km daily	2002–2023	0.58 Pg CO yr <sup>-1 d</sup>	Wiedinmyer et al. (2023)
FEER1	GFAS1.2 FRP & MODIS AOD	0.1° monthly	2003–2013	3.9 Pg C yr <sup>-1 a</sup> 0.56 Pg CO yr <sup>-1 e</sup>	Ichoku and Ellison (2014)
QFED2.5	MODIS & VIIRS FRP & MODIS AOD	0.1° daily	2000–present	0.32 Pg CO yr <sup>-1 e</sup>	Darmenov and da Silva (2015)
	emis. factor				

<sup>a</sup> 2003–2014 average from Li et al. (2024); <sup>b</sup> 2003–2018 average from Pettinari et al. (2025); <sup>c</sup> 2003–2014 average from <https://www.globalfiredata.org/>; <sup>d</sup> 2003–2014 average from Kaiser et al. (2025); <sup>e</sup> 2012–2019 average from Wiedinmyer et al. (2023)



310 For long-term historical trend, we suggest using charcoal-based regional data from the Reading  
 Palaeofire Database (RPD), which is based on records from 1480 sites (Harrison et al., 2022). Also,  
 multi-source merged global gridded fire emission products, such as BB4CMIP5 (Lamarque et al.,  
 2010), BB4CMIP6 (van Marle et al., 2017), and BB4CMIP7 (van Marle and van der Werf, 2025), as  
 well as reconstructed global historical gridded burned area products from Guo et al. (2025) and  
 315 FireCCILT11 (Otón et al., 2021) can be used for comparison with simulations, but they may include  
 larger uncertainties than present-day satellite-based products and RPD.

In addition, regional fire field observations may also serve as valuable benchmarks, e.g., National  
 Interagency Fire Center (NIFC) historical wildfire statistics and Fire Program Analysis Fire-Occurrence  
 Database (FPA FOD) for USA, Canadian National Fire Database (CNFDB), National Forestry and  
 320 Grassland Administration (NFGA) / Ministry of Emergency Management (MEM) annual wildfire  
 statistics and bulletins for China. The above products are recommended but not limited to these.

## 5.2 Fire changes and drivers

We recommend quantifying past, present, and future fire changes using burned area (burntFractionAll)  
 and fire carbon emissions (fFire) from historical/esm-historical and ScenarioMIP experiments (Table 1).  
 325 These changes include, but are not limited to, changes in annual totals, seasonality (timing of fire-season  
 onset and end, fire-season length, peak activity), frequency of extremes, and interannual variation.  
 Because CMIP7 FireMIP will provide multi-model and multi-initial-condition ensembles, uncertainties  
 in fire changes can be explicitly assessed.

Fires are directly regulated by local ecosystem and climate factors, including aboveground  
 330 biomass that sets the fuel load, air humidity and/or soil moisture that determines fuel wetness, wind  
 speed that affects the fire spread rate and indirectly influences fuel wetness, and socio-economic factors  
 (e.g., population density; GDP, land use; forcing data of ESMs) that affect human ignitions and  
 suppressions. By comparing hist-nat, hist-aer, hist-GHG, and hist-lu with historical/esm-historical, the  
 effects of natural forcing, anthropogenic forcing, as well as anthropogenic aerosols, greenhouse gases,  
 335 and land-use changes on local variables and fires can be quantified, and the pathways across Earth  
 system components can be analyzed (Fig. 1). For example, in the Arctic–boreal zone, increasing  
 anthropogenic GHG lead to warming, which can accelerate permafrost thaw and soil drying, thereby



drying fuels and increasing fire risks, inferred from mechanisms described in Kim et al. (2024) and Cai (2024). Comparing the influences of different forcings helps identify the dominant one and pathway.

### 340 5.3 Fire impacts

The influence of fire and fire aerosol emissions could be quantified by comparing outputs from the historical/esm-historical simulations with those from hist-no-fire and hist-no-fireaero, respectively. Specifically, analyses will focus on variables for land–atmosphere–ocean carbon, water, and energy cycles; vegetation composition and structure; fire-induced trace gas and aerosol emissions; atmospheric  
 345 circulation, composition, and chemistry; surface climate (e.g., temperature, humidity, precipitation, and wind speed); cryosphere conditions (e.g., permafrost extent and active-layer thickness, snow and sea-ice extent and depth); ocean physics (currents, temperature, salinity) and marine ecosystems; and human health (based on simulated surface PM<sub>2.5</sub> or O<sub>3</sub> concentrations in ESMs, or calculated outside ESMs using fire carbon emission simulations and atmospheric (chemistry) models). The influence of future fire  
 350 and fire aerosol emission changes could be quantified using scen7-h compared against scen7-h-no-firechange and scen7-h-no-fireaerochange, respectively, with analyses of a similar variable set. Related uncertainties can also be assessed using multi-model and multi-initial-condition ensemble members.

In addition, by quantifying changes in key variables along different pathways and comparing them, the dominant pathway through which fire exerts a statistically significant influence on the target variables  
 355 can be identified. For example, CESM-based estimates show that fire aerosol emissions can affect global precipitation through two pathways: (1) increasing cloud droplet number concentration and thus increasing cloud water path, which tends to reduce precipitation; and (2) fire-aerosol-induced cooling that lowers evaporation and reduces atmospheric water vapor, which also tends to reduce precipitation. Our results show that the reduction in atmospheric water vapor is much stronger than the increase in  
 360 cloud water, indicating that the second pathway is dominant (Fig. 8a in Li et al., 2022).

The full output dataset will support building the first comprehensive picture of global fire’s role in the land–atmosphere–ocean carbon cycle. It will also allow for more accurate and reliable quantification of fire impacts on global and regional climate, benefiting from CMIP7 coupling simulations that incorporate aerosol-cloud interaction modeling, fully coupled ocean models rather than prescribed SSTs  
 365 or slab ocean models, and multi-model, multi-initial-condition ensembles.

## 6 Summary



This paper outlines the protocol for CMIP7 FireMIP, detailing its motivation, experimental design, model inputs and outputs, and recommended analyses.

Previous FireMIP studies provided valuable insights into fire's local drivers and local impacts on vegetation and land carbon dynamics using DGVMs but were limited by offline approaches that could not capture fire-climate and ecosystem-climate interactions. Earlier coupled-model studies lacked either critical climate feedback and processes necessary for accurately quantifying fire impacts or an ensemble framework to support comprehensive uncertainty assessment.

FireMIP's integration into CMIP7 aims to address these limitations by using fully coupled ESMs and a multi-model, multi-initial-condition, and multi-scenario ensemble framework. This allows for a systematic assessment of fire regime changes and fire's interactions with the biosphere, land, atmosphere, hydrosphere, cryosphere, and human systems. By capturing fire response and feedbacks across Earth system components, both local and remote, contemporary and legacy, FireMIP in CMIP7 will provide a more comprehensive understanding of fire's role in the Earth system and improve the scientific basis for fire and environmental management and climate-change mitigation.

CMIP7 aims to answer four science questions: (1) patterns of sea surface change; (2) changing dangerous weather; (3) the water-carbon-climate nexus; and (4) tipping points (Dunne et al., 2025). As the only fire-focused MIP in CMIP7, FireMIP relates to questions (1) and (2) and will help address questions (3) and (4). First, FireMIP can assess how fire-driven aerosol forcing and land-atmosphere flux changes influence large-scale atmospheric circulation and subsequently SST patterns. Second, because fires are closely linked to drought and heatwaves, FireMIP's analysis of fire-regime changes can inform how the associated hazards of changing dangerous weather may evolve. Third, because fire is an integral process linking water, carbon, and climate, FireMIP's assessment of fire drivers and impacts can help clarify interactions among them and inform how the water-carbon-climate nexus may respond to anthropogenic forcings. In addition, fires interact with systems that exhibit tipping-point behavior, such as the Amazon rainforests, boreal forests, permafrost, and Arctic sea ice, so FireMIP can help identify fire-related pathways that may increase the likelihood of abrupt or irreversible transitions.

Updated details on the project and its progress will be available at <https://wcrp-cmip.org/mips/firemip/> (last access: 1 Oct 2025)

*Code and Data availability.*



The protocol paper does not include any code or datasets. The model output from the CMIP7 FireMIP simulations will be distributed through the Earth System Grid Federation (ESGF) and will be freely accessible through ESGF data portals after registration, following standard CMIP7 formats, consistent  
400 with other MIPs within CMIP7.

*Author contribution.*

FL wrote the paper. FL, DL, VKA, BR, HH, MK, RL, ZL, DW, and VA designed the experiments, and FL, YJ, AW, and YL selected the output variables. CL assisted FL in preparing the tables and formatting  
405 the reference list. All authors reviewed and edited the paper.

*Acknowledgements.*

We appreciate the helpful discussions and suggestions on experimental design and output variables from Vivek K. Arora, Keren Mezuman, Jiawen Zhu, Jin-Soo Kim, Zhongwang Wei, Lei Cai, Guangqing Zhou,  
410 Maria Val Martin, Kece Fei, Eleanor O'Rourke, Elisabeth Dingley, Yang Chen, Peter Lawrence, Sam Rabin, Simone Tilmes, Lili Xia, Kazuhisa Tanada, Ian Eisenman, Meinrat O. Andreae, Jong-Seong Kug, Xu Yue, Zehao Shen, Hailong Liu, Pengfei Lin, Yiran Peng, Yong Wang, and Xiaodong Zeng. We also thank the CMIP International Project Office (IPO) for supporting FireMIP, the CMIP Climate Forcings Task Team and input4MIPs for providing CMIP7 forcing data for the experiments, and ESGF for  
415 facilitating the distribution of FireMIP experiment outputs.

*Financial Supports.*

This study is co-supported by the National Key Research and Development Program of China (grant nos. 2022YFE0106500 and 2024YFF0809000), the Guangdong Major Project of Basic and  
420 Applied Basic Research (grant no. 2021B0301030007), and the National Science and Technology Infrastructure project Earth System Science Numerical Simulator Facility (EarthLab). DML is supported by the NSF National Center for Atmospheric Research, which is a major facility sponsored by the U.S. National Science Foundation under Cooperative Agreement No. 1852977. BMR was supported by Google.org and funding catalyzed by the TED Audacious Project (Permafrost Pathways). CB was  
425 supported by the Met Office Hadley Centre Climate Programme funded by DSIT, and the Met Office Climate Science for Service Partnership (CSSP) Brazil project under the International Science



Partnerships Fund (ISPF). HL was supported by the Research Council of Norway project (328922). RL was supported by the Office of Science, U.S. Department of Energy, Biological and Environmental Research as part of the Earth and Environmental Systems Modeling (EESM) Program. PNNL is operated  
 430 for the U.S. DOE by Battelle Memorial Institute for DOE under contract AC05-76RL01830. MK and AV were supported by the Leverhulme Trust through the Leverhulme Centre for Wildfires, Environment and Society, grant number RC-2018-023. AV has also been supported by the AXA Research Fund (project ‘AXA Chair in Wildfires and Climate’, CPO00163217), by the Hellenic Foundation for Research and Innovation (grants FirePC and REINFORCE, with Grant IDs 3453 and 15155, respectively), and by the  
 435 Horizon Europe programme under Grant Agreement No. 101137680 via project CERTAINTY.

#### *Competing interests.*

One author (David M. Lawrence) is a member of the editorial board of GMD.

#### 440 **References**

- Andela, N., Morton, D. C., Giglio, L., Chen, Y., van der Werf, G. R., Kasibhatla, P. S., DeFries, R. S., Collatz, G. J., Hantson, S., Kloster, S., Bachelet, D., Forrest, M., Lasslop, G., Li, F., Mangeon, S., Melton, J. R., Yue, C., and Randerson, J. T.: A human-driven decline in global burned area, *Science*, 356, 1356–1362, <https://doi.org/10.1126/science.aal4108>, 2017.
- 445 Arora, V. K. and Melton, J. R.: Reduction in global area burned and wildfire emissions since 1930s enhances carbon uptake by land, *Nat. Commun.*, 9, 1326, <https://doi.org/10.1038/s41467-018-03838-0>, 2018.
- Beaudor, M., Pouyaei, A., and Wang, R.: How Could Fire Emissions Reshape the Nitrogen Cycle?, *Geophys. Res. Lett.*, published 20 Nov 2025, <https://doi.org/10.1029/2025GL116250>.
- 450 Bhattarai, H., Val Martin, M., Sitch, S., Yung, D. H. Y., and Tai, A. P. K.: Global patterns and drivers of climate-driven fires in a warming world, *EGUsphere* [preprint], <https://doi.org/10.5194/egusphere-2025-804>, 2025.
- Bond-Lamberty, B., Peckham, S. D., Ahl, D. E., and Gower, S. T.: Fire as the dominant driver of central Canadian boreal forest carbon balance, *Nature*, 450, 89–  
 455 92, <https://doi.org/10.1038/nature06272>, 2007.
- Boysen, L. R., Brovkin, V., Pongratz, J., Lawrence, D. M., Lawrence, P., Vuichard, N., Peylin, P., Liddicoat, S., Hajima, T., Zhang, Y., Rocher, M., Delire, C., Séférian, R., Arora, V. K., Nieradzik, L., Anthoni, P., Thiery, W., Laguë, M. M., Lawrence, D., and Lo, M.-H.: Global climate response to idealized deforestation in CMIP6 models, *Biogeosciences*, 17, 5615–5638,  
 460 <https://doi.org/10.5194/bg-17-5615-2020>, 2020.
- Bowman, D. M. J. S., Balch, J. K., Artaxo, P., Bond, W. J., Carlson, J. M., Cochrane, M. A., D’Antonio, C. M., DeFries, R. S., Doyle, J. C., Harrison, S. P., Johnston, F. H., Keeley, J. E., Krawchuk, M.



- A., Kull, C. A., Marston, J. B., Moritz, M. A., Prentice, I. C., Roos, C. I., Scott, A. C., Swetnam, T. W., van der Werf, G. R., and Pyne, S. J.: Fire in the Earth system, *Science*, 324, 481–484, <https://doi.org/10.1126/science.1163886>, 2009.
- Burton, C., Lampe, S., Kelley, D. I., Thiery, W., Hantson, S., Christidis, N., Gudmundsson, L., Forrest, M., Burke, E., Chang, J., Huang, H., Ito, A., Kou-Giesbrecht, S., Lasslop, G., Li, W., Nieradzik, L., Li, F., Chen, Y., Randerson, J., Reyer, C. P. O., and Mengel, M.: Global burned area increasingly explained by climate change, *Nat. Clim. Change*, 14, 1186–1192, <https://doi.org/10.1038/s41558-024-02140-w>, 2024.
- Cai, L., Permafrost thaw as a critical driver of naturally-ignited wildfires in the high latitudes, Workshop: Response and Feedback of Arctic-boreal Permafrost and Wildfires to Climate Change, Beijing, Oct 9–11, 2024.
- Chen, Y., Morton, D. C., Andela, N., van der Werf, G. R., Giglio, L., and Randerson, J. T.: A pan-tropical cascade of fire driven by El Niño/Southern Oscillation, *Nat. Clim. Chang.*, 7, 906–911, <https://doi.org/10.1038/s41558-017-0014-8>, 2017.
- Chen, Y., Romps, D. M., Seeley, J. T., Veraverbeke, S., Riley, W. J., Mekonnen, Z. A., Randerson, J. T.: Future increases in Arctic lightning and fire risk for permafrost carbon, *Nat. Clim. Chang.*, 11, 404–410, <https://doi.org/10.1038/s41558-021-01011-y>, 2021.
- Chen, Y., Hall, J., van Wees, D., Andela, N., Hantson, S., Giglio, L., van der Werf, G. R., Morton, D. C., and Randerson, J. T.: Multi-decadal trends and variability in burned area from the fifth version of the Global Fire Emissions Database (GFED5), *Earth Syst. Sci. Data*, 15, 5227–5259, <https://doi.org/10.5194/essd-15-5227-2023>, 2023.
- Chuvieco, E., Mouillot, F., van der Werf, G. R., San Miguel, J., Tanasse, M., Koutsias, N., García, M., Yebra, M., Padilla, M., Gitas, I., Heili, A., Hawbaker, T. J., and Giglio, L.: Historical background and current developments for mapping burned area from satellite Earth observation, *Remote Sens. Environ.*, 225, 45–64, <https://doi.org/10.1016/j.rse.2019.02.013>, 2019.
- Cunningham, C. X., Abatzoglou, J. T., Kolden, C. A., Williamson, G. J., Steuer, M., Bowman, D. M. J. S.: Climate-linked escalation of societally disastrous wildfires, *Science*, 390, 53–58, <https://doi.org/10.1126/science.adr5127>, 2025.
- Darmenov, A. and da Silva, A.: The Quick Fire Emissions Dataset (QFED): Documentation of versions 2.1, 2.2 and 2.4, NASA Technical Report Series on Global Modeling and Data Assimilation, NASA TM-2015-104606, Volume 38, <http://gmao.gsfc.nasa.gov/pubs/docs/Darmenov796.pdf>, 2015.
- Dunne, J. P., Hewitt, H. T., Arblaster, J. M., Bonou, F., Boucher, O., Cavazos, T., Dingley, B., Durack, P. J., Hassler, B., Juckes, M., Miyakawa, T., Mizielinski, M., Naik, V., Nicholls, Z., O'Rourke, E., Pincus, R., Sanderson, B. M., Simpson, I. R., and Taylor, K. E.: An evolving Coupled Model Intercomparison Project phase 7 (CMIP7) and Fast Track in support of future climate assessment, *Geosci. Model Dev.*, 18, 6671–6700, <https://doi.org/10.5194/gmd-18-6671-2025>, 2025.
- Frieler, K., Volkholz, J., Lange, S., Schewe, J., Mengel, M., del Rocio Rivas López, M., Otto, C., Reyer, C. P. O., Karger, D. N., Malle, J. T., Treu, S., Menz, C., Blanchard, J. L., Harrison, C. S., Petrik, C. M., Eddy, T. D., Ortega-Cisneros, K., Novaglio, C., Rousseau, Y., Watson, R. A., Stock,



- 505 C., Liu, X., Heneghan, R., Tittensor, D., Maury, O., Büchner, M., Vogt, T., Wang, T., Sun, F.,  
 Sauer, I. J., Koch, J., Vanderkelen, I., Jägermeyr, J., Müller, C., Rabin, S., Klar, J., Vega del Valle,  
 I. D., Lasslop, G., Chadburn, S., Burke, E., Gallego-Sala, A., Smith, N., Chang, J., Hantson, S.,  
 Burton, C., Gädeke, A., Li, F., Gosling, S. N., Müller Schmied, H., Hattermann, F., Wang, J., Yao,  
 F., Hickler, T., Marcé, R., Pierson, D., Thiery, W., Mercado-Bettín, D., Ladwig, R., Ayala-Zamora,  
 A. I., Forrest, M., and Bechtold, M.: Scenario setup and forcing data for impact model evaluation  
 and impact attribution within the third round of the Inter-Sectoral Impact Model Intercomparison  
 Project (ISIMIP3a), *Geosci. Model Dev.*, 17, 1–51, <https://doi.org/10.5194/gmd-17-1-2024>, 2024.
- 510 Giglio, L., Boschetti, L., Roy, D. P., Humber, M. L., and Justice, C. O.: The Collection 6 MODIS  
 burned area mapping algorithm and product, *Remote Sens. Environ.*, 217, 72–  
 85, <https://doi.org/10.1016/j.rse.2018.08.005>, 2018.
- 515 Gillett, N. P., Simpson, I. R., Hegerl, G., Knutti, R., Mitchell, D., Ribes, A., Shiogama, H., Stone, D.,  
 Tebaldi, C., Wolski, P., Zhang, W., and Arora, V. K.: The Detection and Attribution Model  
 Intercomparison Project (DAMIP v2.0) contribution to CMIP7, *Geosci. Model Dev.*, 18, 4399–  
 4416, <https://doi.org/10.5194/gmd-18-4399-2025>, 2025.
- Grandey, B. S., Lee, H.-H., and Wang, C.: Radiative effects of interannually varying vs. interannually  
 invariant aerosol emissions from fires, *Atmos. Chem. Phys.*, 16, 14495–  
 14513, <https://doi.org/10.5194/acp-16-14495-2016>, 2016.
- 520 Guo, Z., Li, W., Ciais, P., Sitch, S., van der Werf, G. R., Bowring, S. P. K., Bastos, A., Mouillot, F., He,  
 J., Sun, M., Zhu, L., Du, X., Wang, N., and Huang, X.: Reconstructed global monthly burned area  
 maps from 1901 to 2020, *Earth Syst. Sci. Data*, 17, 3599–3618, <https://doi.org/10.5194/essd-17-3599-2025>, 2025.
- 525 Hamilton, D., Wan, J., Liguori-Bills, N., Kasoar, M., and Hantson, S.: Past and Future Fire Emission  
 Trajectories & Aerosol Radiative Forcing, WCRP-CMIP, [https://wcrp-cmip.org/wp-  
 content/uploads/2024/10/S4\\_DHamilton\\_TO-PUBLISH.pdf](https://wcrp-cmip.org/wp-content/uploads/2024/10/S4_DHamilton_TO-PUBLISH.pdf), 2024.
- 530 Hantson, S., Arneth, A., Harrison, S. P., Kelley, D. I., Prentice, I. C., Rabin, S. S., Archibald, S.,  
 Mouillot, F., Arnold, S. R., Artaxo, P., Bachelet, D., Ciais, P., Forrest, M., Friedlingstein, P.,  
 Hickler, T., Kaplan, J. O., Kloster, S., Knorr, W., Lasslop, G., Li, F., Mangeon, S., Melton, J. R.,  
 Meyn, A., Sitch, S., Spessa, A., van der Werf, G. R., Voulgarakis, A., and Yue, C.: The status and  
 challenge of global fire modelling, *Biogeosciences*, 13, 3359–3375, <https://doi.org/10.5194/bg-13-3359-2016>, 2016.
- 535 Harrison, S. P., Villegas-Díaz, R., Cruz-Silva, E., Gallagher, D., Kesner, D., Lincoln, P., Shen, Y.,  
 Sweeney, L., Colombaroli, D., Ali, A., Barhoumi, C., Bergeron, Y., Blyakharchuk, T., Bobek, P.,  
 Bradshaw, R., Clear, J. L., Czerwiński, S., Daniau, A.-L., Dodson, J., Edwards, K. J., Edwards, M.  
 E., Feurdean, A., Foster, D., Gajewski, K., Gałka, M., Garneau, M., Giesecke, T., Gil Romera, G.,  
 Girardin, M. P., Hofer, D., Huang, K., Inoue, J., Jamrichová, E., Jasiunas, N., Jiang, W., Jiménez-  
 Moreno, G., Karpińska-Kołaczek, M., Kołaczek, P., Kuosmanen, N., Lamentowicz, M., Lavoie,  
 540 M., Li, F., Li, J., Lisitsyna, O., López-Sáez, J. A., Luelmo-Lautenschlaeger, R., Magnan, G.,  
 Magyari, E. K., Maksims, A., Marcisz, K., Marinova, E., Marlon, J., Mensing, S., Miroslaw-  
 Grabowska, J., Oswald, W., Pérez-Díaz, S., Pérez-Obiol, R., Piilo, S., Poska, A., Qin, X., Remy, C.





- C., Richard, P. J. H., Salonen, S., Sasaki, N., Schneider, H., Shotyk, W., Stancikaite, M., Šteinberga, D., Stivrins, N., Takahara, H., Tan, Z., Trasune, L., Umbanhowar, C. E., Väiliranta, M.,  
 545 Vassiljev, J., Xiao, X., Xu, Q., Xu, X., Zawisza, E., Zhao, Y., Zhou, Z., and Paillard, J.: The  
 Reading Palaeofire Database: an expanded global resource to document changes in fire regimes  
 from sedimentary charcoal records, *Earth Syst. Sci. Data*, 14, 1109–  
 1124, <https://doi.org/10.5194/essd-14-1109-2022>, 2022.
- Harrison, S. P., Haas, O., Bartlein, P. J., Sweeney, L., and Zhang, G.: Climate, vegetation, people:  
 550 disentangling the controls of fire at different timescales, *Phil. Trans. R. Soc. B*, 380,  
 20230464, <https://doi.org/10.1098/rstb.2023.0464>, 2025.
- Ichoku, C. and Ellison, L.: Global top-down smoke-aerosol emissions estimation using satellite fire  
 radiative power measurements, *Atmos. Chem. Phys.*, 14, 6643–6667, <https://doi.org/10.5194/acp-14-6643-2014>, 2014.
- 555 IPCC: Climate Change 2021: The Physical Science Basis. Contribution of Working Group I to the  
 Sixth Assessment Report of the Intergovernmental Panel on Climate Change, edited by: Masson-  
 Delmotte, V., Zhai, P., Pirani, A., Connors, S. L., Péan, C., Berger, S., Caud, N., Chen, Y.,  
 Goldfarb, L., Gomis, M. I., Huang, M., Leitzell, K., Lonnoy, E., Matthews, J. B. R., Maycock, T.  
 K., Waterfield, T., Yelekçi, O., Yu, R., and Zhou, B., Cambridge University Press, Cambridge,  
 560 United Kingdom and New York, NY, USA, 2391 pp., 2021.
- Jiang, Y., Lu, Z., Liu, X., Qian, Y., Zhang, K., Wang, Y., and Yang, X.-Q.: Impacts of global open-fire  
 aerosols on direct radiative, cloud and surface-albedo effects simulated with CAM5, *Atmos.*  
*Chem. Phys.*, 16, 14805–14824, <https://doi.org/10.5194/acp-16-14805-2016>, 2016.
- Jiang, Y., Yang, X. Q., Liu, X., Qian, Y., Zhang, K., Wang, M., Li, F., Wang, Y., and Lu, Z.: Impacts of  
 565 wildfire aerosols on global energy budget and climate: The role of climate feedbacks, *J. Clim.*, 33,  
 3351–3366, <https://doi.org/10.1175/JCLI-D-19-0572.1>, 2020.
- Jones, M. W., Abatzoglou, J. T., Veraverbeke, S., Andela, N., Lasslop, G., Forkel, M., Smith, A. J. P.,  
 Burton, C., Betts, R. A., van der Werf, G. R., Sitch, S., Canadell, J. G., Santín, C., Kolden, C.,  
 Doerr, S. H., and Le Q, C.: Global and regional trends and drivers of fire under climate change,  
 570 *Reviews of Geophysics*, 60, e2020RG000726, <https://doi.org/10.1029/2020RG000726>, 2022.
- Kaiser, J. W., Heil, A., Andreae, M. O., Benedetti, A., Chubarova, N., Jones, L., Morcrette, J.-J.,  
 Razinger, M., Schultz, M. G., Suttie, M., and van der Werf, G. R.: Biomass burning emissions  
 estimated with a global fire assimilation system based on observed fire radiative power,  
*Biogeosciences*, 9, 527–554, <https://doi.org/10.5194/bg-9-527-2012>, 2012.
- 575 Kaiser, J., Huijnen, V., Remy, S., Ytre-Eide, M. A., De Jong, M. C., Zheng, B., and Wiedinmyer, C.:  
 Evaluation of fire emissions for HTAP3 with CAMS GFAS and IFS-COMPO, EGU General  
 Assembly 2025, Vienna, Austria, 27 Apr–2 May 2025, EGU25-  
 8708, <https://doi.org/10.5194/egusphere-egu25-8708>, 2025.
- Kaiser, J. and Holmedal, D. G.: GFAS4HTAPv1.2.1 vegetation fire emissions 2003-2023 (Beta),  
 580 Zenodo [data set], <https://doi.org/10.5281/zenodo.13753452>, 2024.
- Kay, J. E., Deser, C., Phillips, A., Mai, A., Hannay, C., Strand, G., Arblaster, J. M., Bates, S. C.,  
 Danabasoglu, G., Edwards, J., Holland, M., Kushner, P., Lamarque, J.-F., Lawrence, D., Lindsay,



- 585 K., Middleton, A., Munoz, E., Neale, R., Oleson, K., Polvani, L., and Vertenstein, M.: The  
 Community Earth System Model (CESM) Large Ensemble Project: a community resource for  
 studying climate change in the presence of internal climate variability, *B. Am. Meteorol. Soc.*, 96,  
 1333–1349, <https://doi.org/10.1175/bams-d-13-00255.1>, 2015.
- Kim, I.-W., Timmermann, A., Kim, J.-E., Rodgers, K. B., Lee, S.-S., Lee, H., and Wieder, W. R.:  
 Abrupt increase in Arctic–Subarctic wildfires caused by future permafrost thaw, *Nat. Commun.*,  
 15, 7868, <https://doi.org/10.1038/s41467-024-51447-4>, 2024.
- 590 Kim, J.-S., Kug, J.-S., Jeong, S.-J., Park, H., and Schaepman-Strub, G.: Extensive fires in southeastern  
 Siberian permafrost linked to preceding Arctic Oscillation, *Sci. Adv.*, 6, eaax3308,  
<https://doi.org/10.1126/sciadv.aax3308>, 2020.
- Kloster, S. and Lasslop, G.: Historical and future fire occurrence (1850 to 2100) simulated in CMIP5  
 Earth System Models, *Global Planet. Change*, 150, 58–69,  
 595 <https://doi.org/10.1016/j.gloplacha.2016.12.017>, 2017.
- Lamarque, J.-F., Bond, T. C., Eyring, V., Granier, C., Heil, A., Klimont, Z., Lee, D., Liousse, C.,  
 Mieville, A., Owen, B., Schultz, M. G., Shindell, D., Smith, S. J., Stehfest, E., Van Aardenne, J.,  
 Cooper, O. R., Kainuma, M., Mahowald, N., McConnell, J. R., Naik, V., Riahi, K., and van  
 Vuuren, D. P.: Historical (1850–2000) gridded anthropogenic and biomass burning emissions of  
 600 reactive gases and aerosols: methodology and application, *Atmos. Chem. Phys.*, 10, 7017–  
 7039, <https://doi.org/10.5194/acp-10-7017-2010>, 2010.
- Landry, J.-S., Partanen, A.-I., and Matthews, H. D.: Carbon cycle and climate effects of forcing from  
 fire-emitted aerosols, *Environ. Res. Lett.*, 12, 025002, <https://doi.org/10.1088/1748-9326/aa51de>,  
 2017.
- 605 Lasslop, G., Coppola, A. I., Voulgarakis, A., Yue, C., and Veraverbeke, S.: Influence of Fire on the  
 Carbon Cycle and Climate, *Curr. Clim. Change Rep.*, 5, 112–123, <https://doi.org/10.1007/s40641-019-00128-9>, 2019.
- Lasslop, G., Hantson, S., Harrison, S. P., Bachelet, D., Burton, C., Forkel, M., Forrest, M., Li, F.,  
 Melton, J. R., Yue, C., Archibald, S., Scheiter, S., Arneth, A., Hickler, T., and Sitch, S.: Global  
 610 ecosystems and fire: Multi-model assessment of fire-induced tree-cover and carbon storage  
 reduction, *Global Change Biology*, 26, 5027–5041, <https://doi.org/10.1111/gcb.15160>, 2020.
- Lenton, T. M., Rockström, J., Gaffney, O., Rahmstorf, S., Richardson, K., Steffen, W., and  
 Schellnhuber, H. J.: Climate tipping points – too risky to bet against, *Nature*, 575, 592–595,  
<https://doi.org/10.1038/d41586-019-03595-0>, 2019.
- 615 Li, F.: Quantifying the impacts of fire aerosols on global terrestrial ecosystem productivity with the  
 fully-coupled Earth system model CESM, *Atmos. Oceanic Sci. Lett.*, 13, 330–337,  
<https://doi.org/10.1080/16742834.2020.1740580>, 2020.
- Li, F.: Fires in CMIP6 models, 2021 FireMIP workshop, Zoom, Nov 9, 2021.
- Li, F., Bond-Lamberty, B., and Levis, S.: Quantifying the role of fire in the Earth system – Part 2:  
 620 Impact on the net carbon balance of global terrestrial ecosystems for the 20th century,  
*Biogeosciences*, 11, 1345–1360, <https://doi.org/10.5194/bg-11-1345-2014>, 2014.
- Li, F. and Lawrence, D. M.: Role of fire in the global land water budget during the 20th century



- through changing ecosystems, *J. Clim.*, 30, 1893–1908, <https://doi.org/10.1175/JCLI-D-16-0460.1>, 2017a.
- 625 Li, Fang, Lawrence, D. M., Bond-Lamberty, B.: Human impacts on 20th century fire dynamics and implications for global carbon and water trajectories, *Glob. Planet. Change*, 162, 18–27, <http://dx.doi.org/10.1016/j.gloplacha.2018.01.002>, 2018.
- Li, F., Lawrence, D. M., and Bond-Lamberty, B.: Impact of fire on global land surface air temperature and energy budget for the 20th century due to changes within ecosystems, *Environ. Res. Lett.*, 12, 044014, <https://doi.org/10.1088/1748-9326/aa6685>, 2017b.
- 630 Li, F., Lawrence, D. M., Jiang, Y., Liu, X., and Lin, Z.: Fire aerosols slow down the global water cycle, *J. Clim.*, 35, 3619–3633, <https://doi.org/10.1175/JCLI-D-21-0245.1>, 2022.
- Li, F., Song, X., Harrison, S. P., Marlon, J. R., Lin, Z., Leung, L. R., Schwinger, J., Marécal, V., Wang, S., Ward, D. S., Dong, X., Lee, H., Nieradzik, L., Rabin, S. S., and Séférian, R.: Evaluation of
- 635 global fire simulations in CMIP6 Earth system models, *Geosci. Model Dev.*, 17, 8751–8771, <https://doi.org/10.5194/gmd-17-8751-2024>, 2024.
- Li, F., Val Martin, M., Andreae, M. O., Arneth, A., Hantson, S., Kaiser, J. W., Lasslop, G., Yue, C., Bachelet, D., Forrest, M., Kluzek, E., Liu, X., Mangeon, S., Melton, J. R., Ward, D. S., Darmenov, A., Hickler, T., Ichoku, C., Magi, B. I., Sitch, S., van der Werf, G. R., Wiedinmyer, C., and Rabin, S. S.: Historical (1700–2012) global multi-model estimates of the fire emissions from the Fire
- 640 Modeling Intercomparison Project (FireMIP), *Atmos. Chem. Phys.*, 19, 12545–12567, <https://doi.org/10.5194/acp-19-12545-2019>, 2019.
- Li, F., Levis, S., and Ward, D. S.: Quantifying the role of fire in the Earth system – Part 1: Improved global fire modeling in the Community Earth System Model (CESM1), *Biogeosciences*, 10, 2293–
- 645 2314, <https://doi.org/10.5194/bg-10-2293-2013>, 2013.
- Lizundia-Loiola, J., Franquesa, M., Khairoun, A., and Chuvieco, E.: Global burned area mapping from Sentinel-3 Synergy and VIIRS active fires, *Remote Sens. Environ.*, 282, 113298, <https://doi.org/10.1016/j.rse.2022.113298>, 2022.
- Lou, S., Liu, Y., Bai, Y., Li, F., Lin, G., Xu, L., Liu, Z., Chen, Y., Dong, X., Zhao, M., Wang, L., Jin, M., Wang, C., Cai, W., Gong, P., and Luo, Y.: Projections of mortality risk attributable to short-term exposure to landscape fire smoke in China, 2021–2100: A health impact assessment study, *Lancet Planet. Health*, 7, e841–e849, [https://doi.org/10.1016/S2542-5196\(23\)00192-4](https://doi.org/10.1016/S2542-5196(23)00192-4), 2023.
- Mao, J.: Fires jeopardize world’s carbon sink, *Nat. Geosci.* 17, 1072–1073, <https://doi.org/10.1038/s41561-024-01562-7>, 2024.
- 655 Oberhagemann, L., Billing, M., von Bloh, W., Drüke, M., Forrest, M., Bowring, S. P. K., Hetzer, J., Ribalaygua Batalla, J., and Thonicke, K.: Sources of uncertainty in the SPITFIRE global fire model: development of LPJmL-SPITFIRE1.9 and directions for future improvements, *Geosci. Model Dev.*, 18, 2021–2050, <https://doi.org/10.5194/gmd-18-2021-2025>, 2025.
- Otón, G., Lizundia-Loiola, J., Pettinari, M. L., and Chuvieco, E.: Development of a consistent global
- 660 long-term burned area product (1982–2018) based on AVHRR-LTDR data, *Int. J. Appl. Earth Obs. Geoinf.*, 103, 102473, <https://doi.org/10.1016/j.jag.2021.102473>, 2021.
- Park, C., Takahashi, K., Fujimori, S., Phung, V., Li, F., Takakura, J., Hasegawa, T., and Jansakoo, T.:



- Future fire-PM<sub>2.5</sub> mortality varies depending on climate and socioeconomic changes, *Environ. Res. Lett.*, 19, 024003, <https://doi.org/10.1088/1748-9326/ad1b7d>, 2024.
- 665 Pellegrini, A. F. A., Reich, P. B., Hobbie, S. E., Coetsee, C., Wigley, B., February, E., Georgiou, K.,  
 Terror, C., Brookshire, E. N. J., and Ahlström, A.: Soil carbon storage capacity of drylands under  
 altered fire regimes, *Nat. Clim. Chang.*, 13, 1089–1094, <https://doi.org/10.1038/s41558-023-01800-7>, 2023.
- 670 Pettinari, M. L., Khairoun, A., Torres-Vázquez, M. Á., Storm, T., Boettcher, M., and Chuvieco, E.:  
 FireCCI Burned Area Algorithms and Products for Climate Modelling, *Living Planet Symposium*,  
 Vienna, Austria, 23–27 June 2025.
- Rabin, S. S., Melton, J. R., Lasslop, G., Bachelet, D., Forrest, M., Hantson, S., Kaplan, J. O., Li, F.,  
 Mangeon, S., Ward, D. S., Yue, C., Arora, V. K., Hickler, T., Kloster, S., Knorr, W., Nieradzik, L.,  
 Spessa, A., Folberth, G. A., Sheehan, T., Voulgarakis, A., Kelley, D. I., Prentice, I. C., Sitch, S.,  
 675 Harrison, S., and Arneeth, A.: The Fire Modeling Intercomparison Project (FireMIP), phase 1:  
 experimental and analytical protocols with detailed model descriptions, *Geosci. Model Dev.*, 10,  
 1175–1197, <https://doi.org/10.5194/gmd-10-1175-2017>, 2017.
- Randerson, J. T., Liu, H., Flanner, M. G., Chambers, S. D., Jin, Y., Hess, P. G., Pfister, G., Mack, M. C.,  
 Treseder, K. K., Welp, L. R., and Chapin, F. S.: The impact of boreal forest fire on climate  
 680 warming, *Science*, 314, 1130–1132, <https://doi.org/10.1126/science.1132075>, 2006.
- Sayedi, S. S., Abbott, B. W., Vannière, B., Leys, B., Colombaroli, D., Romera, G. G., Słowiński, M.,  
 Aleman, J. C., Blarquez, O., Feurdean, A., and Brown, K.: Assessing changes in global fire  
 regimes, *Fire Ecol.*, 20, 18, <https://doi.org/10.1186/s42408-023-00237-9>, 2024.
- Scholten, R. C., Pendergrass, A. G., Abatzoglou, J. T., Xu, C., and Tchepakova, N. M.: Early snowmelt  
 685 and polar jet dynamics co-influence recent extreme Siberian fire seasons, *Science*, **378**, 1005–  
 1009, <https://doi.org/10.1126/science.abn4419>, 2022.
- Scholten, R. C., Veraverbeke, S., Chen, Y., and Randerson, J. T.: Spatial variability in Arctic–boreal fire  
 regimes influenced by environmental and human factors, *Nat. Geosci.*, 17, 866–  
 873, <https://doi.org/10.1038/s41561-024-01505-2>, 2024.
- 690 Scholze, M., Allen, J. I., Collins, W. J., Cornell, S. E., Huntingford, C., Joshi, M., Lowe, J. A., Smith,  
 R. S., and Wild, O.: Earth system models: a tool to understand changes in the Earth system, in:  
 Understanding the Earth System. *Global Change Science for Applications*, edited by: Cornell, S.  
 E., Prentice, I. C., House, J. I., and Downy, C. J., Cambridge University Press, Cambridge, 129–  
 159, 2013.
- 695 Scott, A. C. and Glasspool, I. J.: The diversification of Palaeozoic fire systems and fluctuations in  
 atmospheric oxygen concentration, *Proceedings of the National Academy of Sciences. USA*, 103,  
 10861–10865, <https://doi.org/10.1073/pnas.0604090103>, 2006.
- Seo, H. and Kim, Y.: Forcing the Global Fire Emissions Database burned-area dataset into the  
 Community Land Model version 5.0: impacts on carbon and water fluxes at high latitudes, *Geosci.*  
 700 *Model Dev.*, 16, 4699–4713, <https://doi.org/10.5194/gmd-16-4699-2023>, 2023.
- Teckentrup, L., Harrison, S. P., Hantson, S., Heil, A., Melton, J. R., Forrest, M., Li, F., Yue, C., Arneeth,  
 A., Hickler, T., Sitch, S., and Lasslop, G.: Response of simulated burned area to historical changes



- in environmental and anthropogenic factors: a comparison of seven fire models, *Biogeosciences*,  
 16, 3883–3910, <https://doi.org/10.5194/bg-16-3883-2019>, 2019.
- 705 Teixeira, J. C. M., Burton, C., Kelley, D. I., Folberth, G. A., O'Connor, F. M., Betts, R. A., and  
 Voulgarakis, A.: Improving historical trends in the INFERNO fire model using the Human  
 Development Index, *EGUsphere* [preprint], <https://doi.org/10.5194/egusphere-2025-3066>, 2025.
- Tian, C., Yue, X., Zhu, J., Liao, H., Yang, Y., Lei, Y., Zhou, X., Zhou, H., Ma, Y., and Cao, Y.: Fire–  
 climate interactions through the aerosol radiative effect in a global chemistry–climate–vegetation  
 710 model, *Atmos. Chem. Phys.*, 22, 12353–12366, <https://doi.org/10.5194/acp-22-12353-2022>, 2022.
- Tian, H., Lu, C., Ciais, P., Michalak, A. M., Canadell, J. G., Saikawa, E., Huntzinger, D. N., Gurney, K.  
 R., Sitch, S., Zhang, B., Yang, J., Bousquet, P., Bruhwiler, L., Chen, G., Dlugokencky, E.,  
 Friedlingstein, P., Melillo, J., Pan, S., Poulter, B., Prinn, R., Saunois, M., Schwalm, C. R., and  
 Wofsy, S. C.: The terrestrial biosphere as a net source of greenhouse gases to the atmosphere,  
 715 *Nature*, 531, 225–228, <https://doi.org/10.1038/nature16946>, 2016.
- Tosca, M. G., Randerson, J. T., and Zender, C. S.: Global impact of smoke aerosols from landscape  
 fires on climate and the Hadley circulation, *Atmos. Chem. Phys.*, 13, 5227–5241,  
<https://doi.org/10.5194/acp-13-5227-2013>, 2013.
- United Nations Environment Programme (UNEP): Spreading like Wildfire – The Rising Threat of  
 720 Extraordinary Landscape Fires, A UNEP Rapid Response Assessment, Nairobi, 126  
 pp., [https://www.unep.org/resources/report/spreading-wildfire-rising-threat-extraordinary-  
 landscape-fires](https://www.unep.org/resources/report/spreading-wildfire-rising-threat-extraordinary-landscape-fires), 2022.
- van der Werf, G. R., Randerson, J. T., Giglio, L., van Leeuwen, T. T., Chen, Y., Rogers, B. M., Mu, M.,  
 van Marle, M. J. E., Morton, D. C., Collatz, G. J., Yokelson, R. J., and Kasibhatla, P. S.: Global  
 725 fire emissions estimates during 1997–2016, *Earth Syst. Sci. Data*, 9, 697–  
 720, <https://doi.org/10.5194/essd-9-697-2017>, 2017.
- van Marle, M. J. E., Kloster, S., Magi, B. I., Marlon, J. R., Daniau, A.-L., Field, R. D., Arneth, A.,  
 Forrest, M., Hantson, S., Kehrwald, N. M., Knorr, W., Lasslop, G., Li, F., Mangeon, S., Yue, C.,  
 Kaiser, J. W., and van der Werf, G. R.: Historic global biomass burning emissions for CMIP6  
 730 (BB4CMIP) based on merging satellite observations with proxies and fire models (1750–2015),  
*Geosci. Model Dev.*, 10, 3329–3357, <https://doi.org/10.5194/gmd-10-3329-2017>, 2017.
- van Marle, M. J. E. and van der Werf, G. R.: DRES-CMIP-BB4CMIP7-2-0, [https://input4mips-  
 cvs.readthedocs.io/en/latest/source-id-landing-pages/DRES-CMIP-BB4CMIP7-2-0/](https://input4mips-cvs.readthedocs.io/en/latest/source-id-landing-pages/DRES-CMIP-BB4CMIP7-2-0/), (last access:  
 10 October 2025), 2025.
- 735 van Vuuren, D., O'Neill, B., Tebaldi, C., Chini, L., Friedlingstein, P., Hasegawa, T., Riahi, K.,  
 Sanderson, B., Govindasamy, B., Bauer, N., Eyring, V., Fall, C., Frieler, K., Gidden, M., Gohar,  
 L., Jones, A., King, A., Knutti, R., Kriegler, E., Lawrence, P., Lennard, C., Lowe, J., Mathison, C.,  
 Mehmood, S., Prado, L., Zhang, Q., Rose, S., Ruane, A., Schleussner, C.-F., Seferian, R.,  
 Sillmann, J., Smith, C., Sörensson, A., Panickal, S., Tachiiri, K., Vaughan, N., Vishwanathan, S.,  
 740 Yokohata, T., and Ziehn, T.: The Scenario Model Intercomparison Project for CMIP7  
 (ScenarioMIP-CMIP7), *EGUsphere* [preprint], <https://doi.org/10.5194/egusphere-2024-3765>,  
 2025.



- Verjans, V., Franzke, C. L. E., Lee, S., Kim, I., Tilmes, S., Lawrence, D. M., Vitt, F., and Li, F.: Quantifying CO<sub>2</sub> forcing effects on lightning, wildfires, and climate interactions, *Sci. Adv.*, 11, eadt5088, <https://doi.org/10.1126/sciadv.adt5088>, 2025.
- 745 Ward, D. S., Kloster, S., Mahowald, N. M., Rogers, B. M., Randerson, J. T., and Hess, P. G.: The changing radiative forcing of fires: global model estimates for past, present and future, *Atmos. Chem. Phys.*, 12, 10857–10886, <https://doi.org/10.5194/acp-12-10857-2012>, 2012.
- Ward, D. S., Shevliakova, E., Malyshev, S., and Rabin, S.: Trends and variability of global fire emissions due to historical anthropogenic activities, *Global Biogeochem. Cy.*, 32, 122–142, <https://doi.org/10.1002/2017GB005787>, 2018.
- 750 Whaley, C. H., Butler, T., Adame, J. A., Ambulkar, R., Arnold, S. R., Buchholz, R. R., Gaubert, B., Hamilton, D. S., Huang, M., Hung, H., Kaiser, J. W., Kaminski, J. W., Knote, C., Koren, G., Kouassi, J.-L., Lin, M., Liu, T., Ma, J., Manomaiphiboon, K., Bergas Masso, E., McCarty, J. L., Mertens, M., Parrington, M., Peiro, H., Saxena, P., Sonwani, S., Surapipith, V., Tan, D. Y. T., Tang, W., Tanpipat, V., Tsigaridis, K., Wiedinmyer, C., Wild, O., Xie, Y., and Zuidema, P.: HTAP3 Fires: towards a multi-model, multi-pollutant study of fire impacts, *Geosci. Model Dev.*, 18, 3265–3309, <https://doi.org/10.5194/gmd-18-3265-2025>, 2025.
- Wiedinmyer, C., Kimura, Y., McDonald-Buller, E. C., Emmons, L. K., Buchholz, R. R., Tang, W., Seto, K., Joseph, M. B., Barsanti, K. C., Carlton, A. G., and Yokelson, R.: The Fire Inventory from NCAR version 2.5: an updated global fire emissions model for climate and chemistry applications, *Geosci. Model Dev.*, 16, 3873–3891, <https://doi.org/10.5194/gmd-16-3873-2023>, 2023.
- 760 Wu, C., Sitch, S., Huntingford, C., Mercado, L. M., Venevsky, S., Lasslop, G., Archibald, S., and Staver, A. C.: Reduced global fire activity due to human demography slows global warming by enhanced land carbon uptake, *P. Natl. Acad. Sci. USA*, 119, e2101186119, <https://doi.org/10.1073/pnas.2101186119>, 2022.
- Xu, L., Zhu, Q., Riley, W. J., Chen, Y., Wang, H.-L., Ma, P.-L., and Randerson, J. T.: The Influence of Fire Aerosols on Surface Climate and Gross Primary Production in the Energy Exascale Earth System Model (E3SM), *J. Clim.*, 34, 7219–7238, <https://doi.org/10.1175/JCLI-D-21-0193.1>, 2021.
- 770 Yu, Y. and Ginoux, P.: Enhanced dust emission following large wildfires due to vegetation disturbance, *Nat. Geosci.*, 15, 878–884, <https://doi.org/10.1038/s41561-022-01046-6>, 2022.
- Yu, Y., Mao, J., Wullschleger, S. D., Chen, A., Shi, X., Wang, Y., Hoffman, F. M., Zhang, Y., and Pierce, E.: Machine learning–based observation-constrained projections reveal elevated global socioeconomic risks from wildfire, *Nat. Commun.*, 13, 1250, <https://doi.org/10.1038/s41467-022-28853-0>, 2022.
- 775 Yue, X. and Unger, N.: Fire air pollution reduces global terrestrial productivity, *Nat. Commun.*, 9, 5413, <https://doi.org/10.1038/s41467-018-07921-4>, 2018.
- Zhao, S. and Suzuki, K.: Differing Impacts of Black Carbon and Sulfate Aerosols on Global Precipitation and the ITCZ Location via Atmosphere and Ocean Energy Perturbations, *J. Clim.*, 32, 5567–5582, <https://doi.org/10.1175/JCLI-D-19-0001.1>, 2019.
- 780 Zhao, Z., Lin, Z., Li, F., and Rogers, B. M.: Influence of Atmospheric Teleconnections on Interannual Variability of Arctic-Boreal Fires, *Sci. Total Environ.*, 838,



- 156550, <https://doi.org/10.1016/j.scitotenv.2022.156550>, 2022.
- 785 Zheng, B., Ciais, P., Chevallier, F., Chuvieco, E., Chen, Y., and Yang, H.: Increasing forest fire  
emissions despite the decline in global burned area, *Sci. Adv.*, 7,  
eabh2646, <https://doi.org/10.1126/sciadv.abh2646>, 2021.
- Zhong, Q., Schutgens, N., Veraverbeke, S., et al.: Increasing aerosol emissions from boreal biomass  
burning exacerbate Arctic warming, *Nat. Clim. Change*, 14, 1275–  
1281, <https://doi.org/10.1038/s41558-024-02176-y>, 2024.
- 790 Zou, Y., Wang, Y., Qian, Y., Tian, H., Yang, J., and Alvarado, E.: Using CESM-RESFire to understand  
climate–fire–ecosystem interactions and the implications for decadal climate variability, *Atmos.  
Chem. Phys.*, 20, 995–1020, <https://doi.org/10.5194/acp-20-995-2020>, 2020.